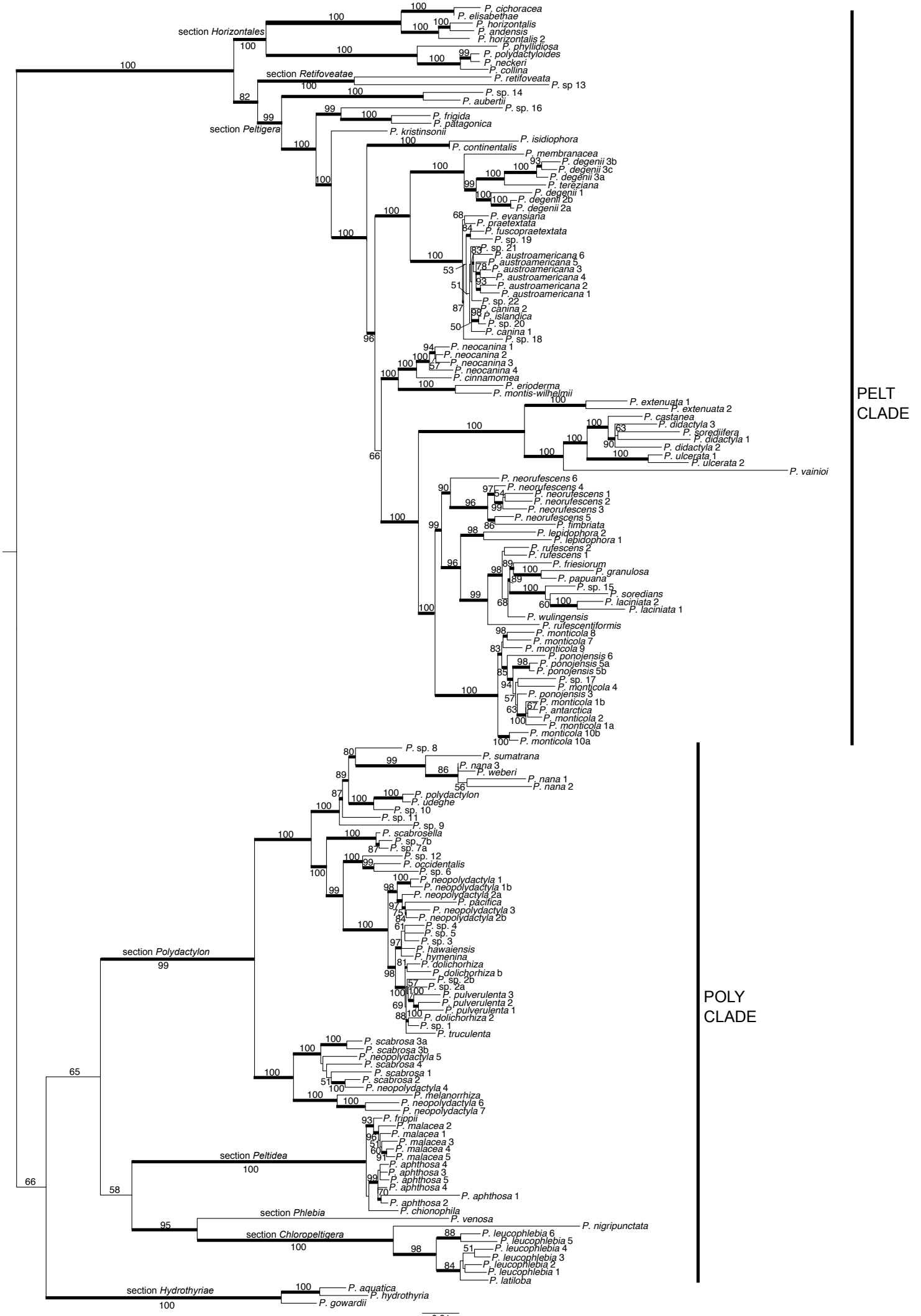

Figure S1. Maximum likelihood tree of the genus *Peltigera* based on seven loci and 175 OTUs representing validated species. The tree was rooted using *Solorina* and *Nephroma* species as the outgroup (not shown). Values above or below branches represent bootstrap support (BS). BS values under 50 are not shown. Thick branches have BS > 70. PELT and POLY clades as shown in Fig 2 are indicated by vertical bars on the right side of the tree. Scale represents nucleotide substitutions per site.

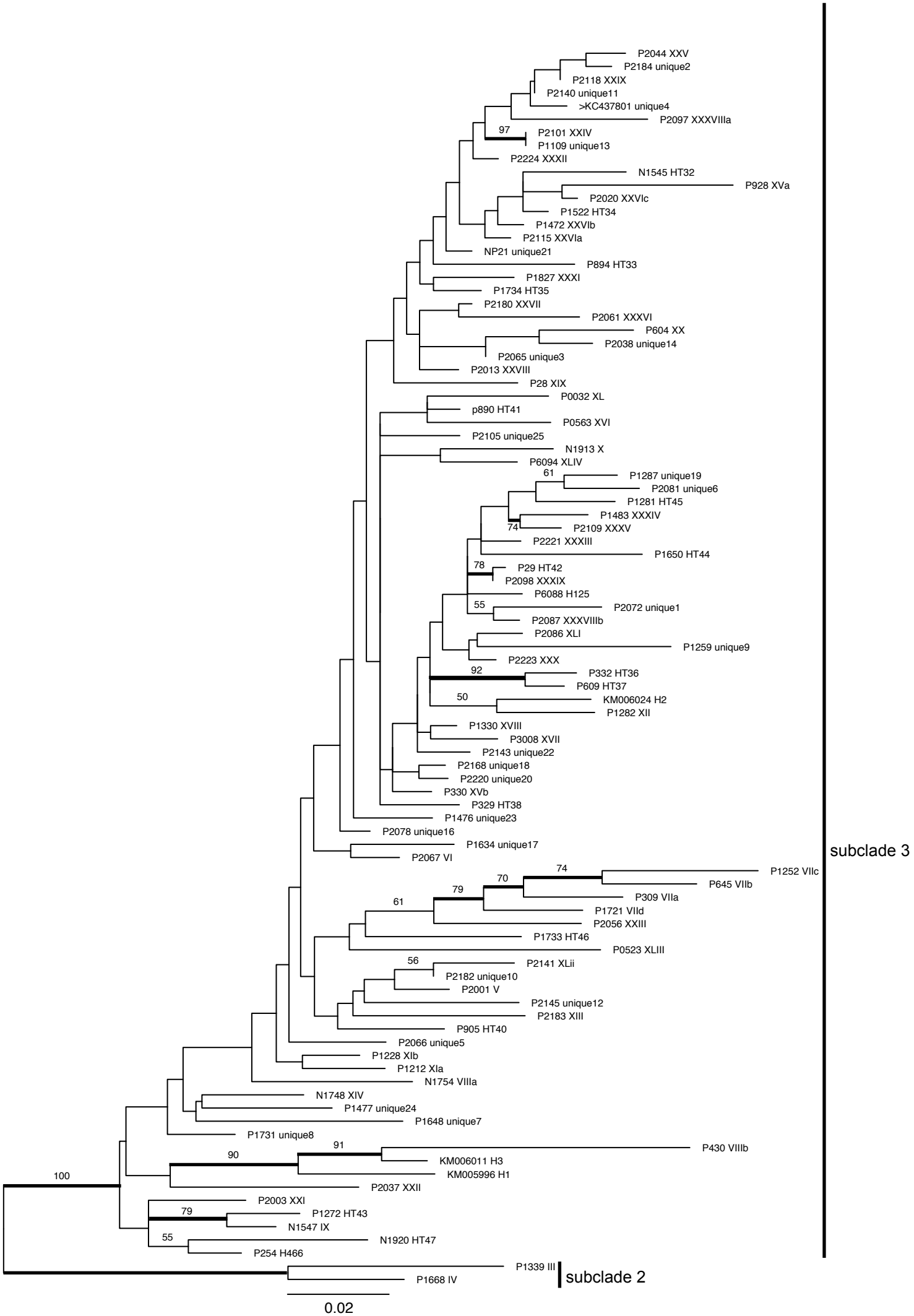

Figure S2. Maximum likelihood tree of *Nostoc* clade II phylogroups and haplotypes associated with *Peltigera*, based on *rbcLX*. Rooting of the tree follows Magain et al. (2017a). Values above or below branches represent bootstrap support (BS). BS values under 50 are not shown. Thick branches have BS > 70. Subclades 2 and 3 are indicated by vertical bars on the right side of the tree. Scale represents nucleotide substitutions per site.

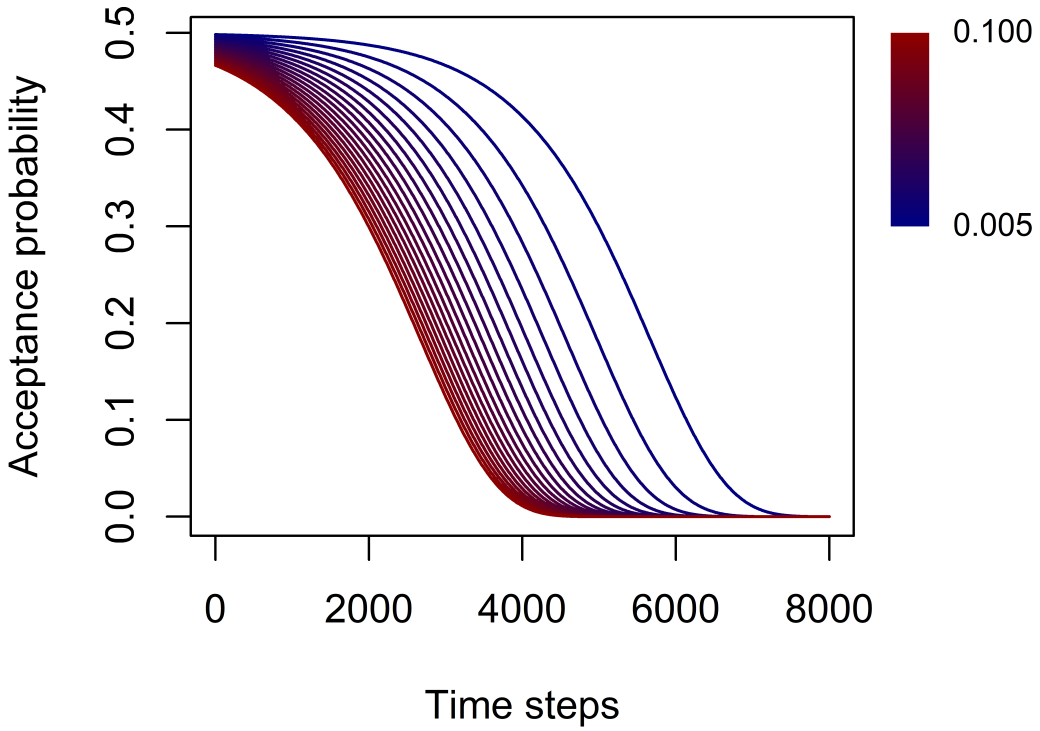

Figure S3. Probability of acceptance of a given module swap as a function of (1) the time step during the algorithm (x-axis) and (2) the magnitude of its negative impact on modularity *Q* (here showing a gradient from decreasing *Q* by 0.100 [red] to decreasing *Q* by 0.005 [blue]). We see that during the cooling of the algorithm, swaps having a negative impact on *Q* have an increasingly low probability of being accepted. Swaps having a positive impact on *Q* are not shown here, because they always have a probability of 1 of being accepted.

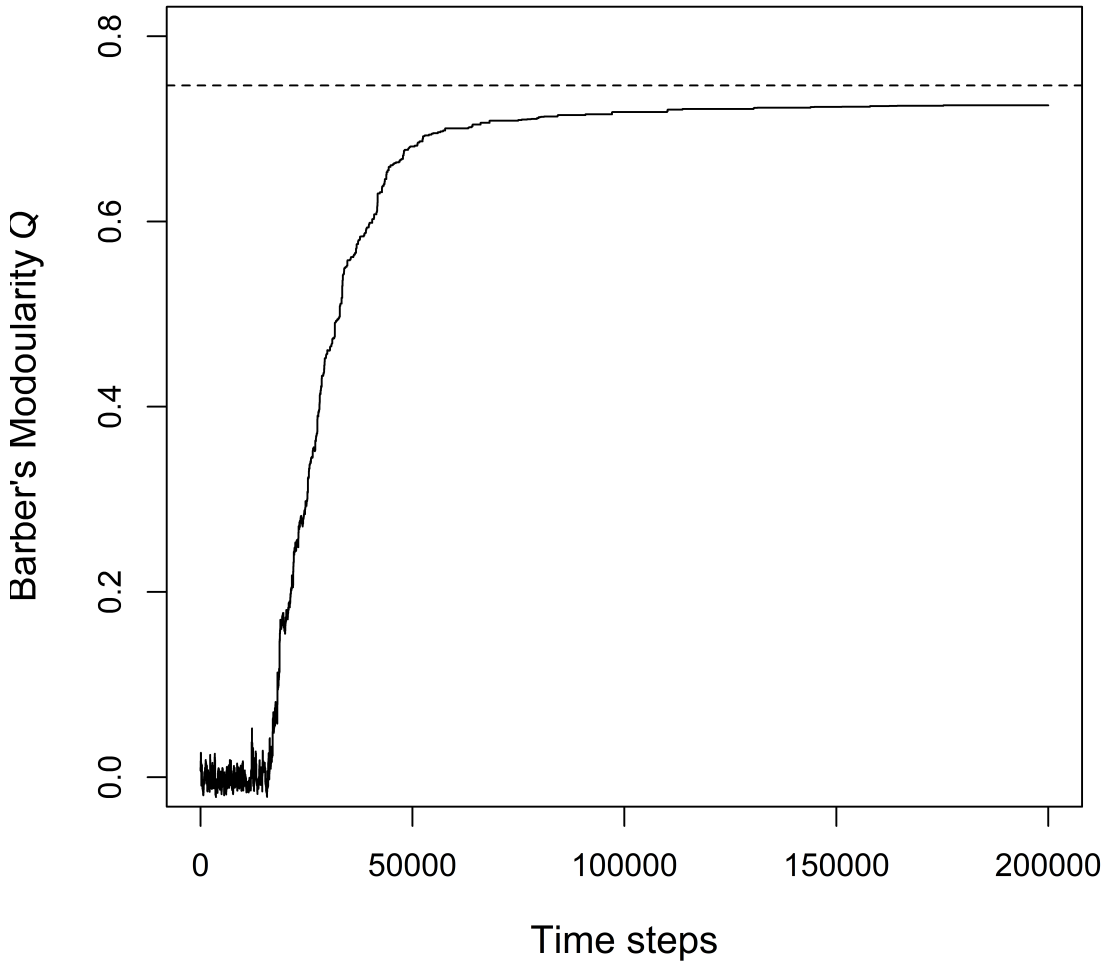

Figure S4. Convergence of our modularity algorithm. We plot the modularity *Q* along the time steps during our algorithm. We clearly see the intiial "hot-phase" of the algorithm with low and widely fluctuating *Q* values, and the progressive cooling of the chain towards slow convergence to an optimal module configuration. This algorithm converged at a modularity value of 0.726. This is quite similar to the value typically reached by trials using the algorithm of Beckett (2016, https://doi.org/10.1098/rsos.140536) implemented in the R package *bipartite* (0.732). However, we manually looked at every module and found some inconsistencies (e.g., mycobiont not in the same module of its sole cyanobiont partner). Manually reassigning these artefacts yielded a *Q* value of 0.747 (dashed line on the graph). However, given the large size of our network, it was not computationally possible to reach this optimal value in a reasonable time frame.

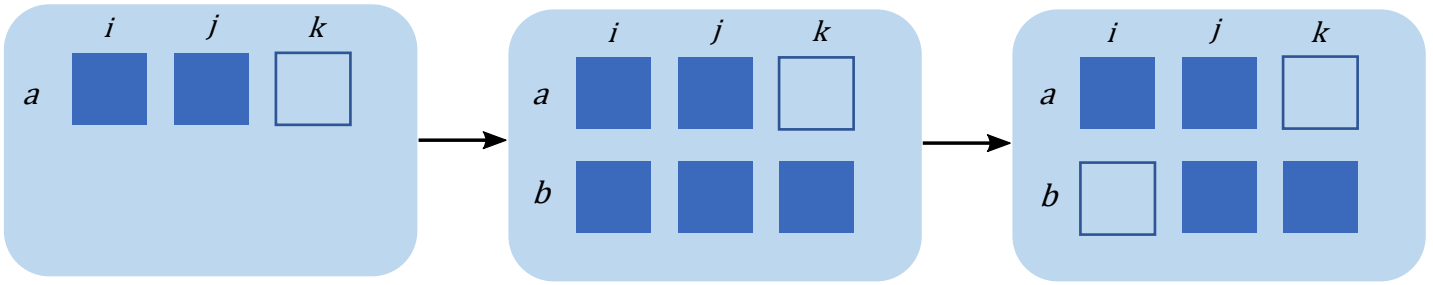

$S = 0.67$
$D = 0.33$
$R = 0$

$S = 0.67$
$D = 0$
$R = 0.33$

Figure S5. Graphical representation of a fungal speciation event driven by an initial partner gain, and the loss of one ancestral partner. Simple calculations show that initially the partner gain drives a high *D*-component, while the loss of one ancestral partner rather drives the *R*-component to become large. Thus, the balance between the *D* and *R* components in beta-diversity, or SDR analyses, may depend upon the time since divergence when comparing sister species, if ever this pattern of partner gain and loss is respected in nature.

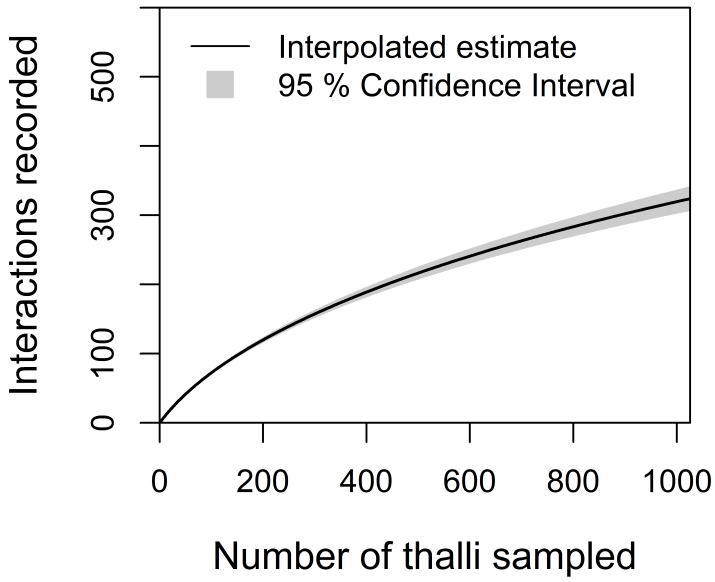

Figure S6. Interaction rarefaction curve. Following the method of Chao et al. (2014) based on Hill numbers, we generated an interaction rarefaction curve interpolating the number of interactions recorded according to our sampling effort. We used order q = 0, and this analysis yielded an estimate of 594 total interactions that might have been recorded through an exhaustive sampling scheme. In our study, we recorded 324.

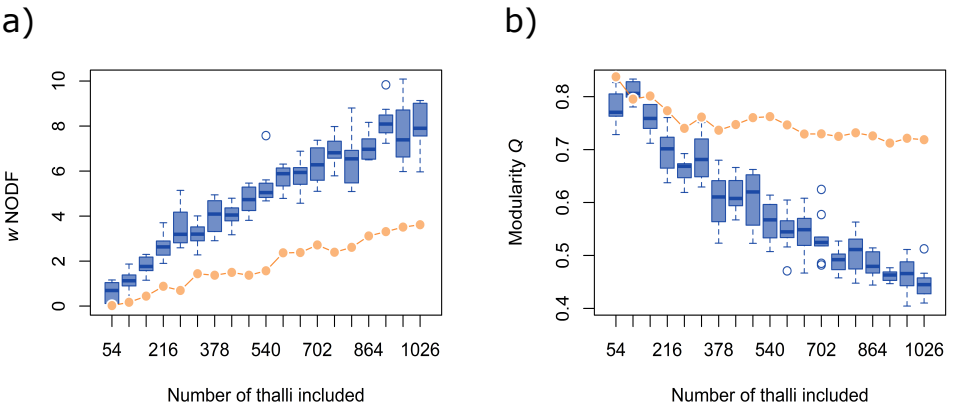

Figure S7. Nestedness (a) and modularity (b) rarefaction curves. On each panel, the *x*-axis represents an intensity of network resampling (up to including the 1026 thalli of our full dataset). The orange circles represent the observed for each rarefied network, and the boxplots represent the (a) nestedness (*w*NODF) or (b) modularity *Q* of 10 random matrices generated for each respective rarefied network using a probabilistic null model that preserved network connectance and marginal totals.

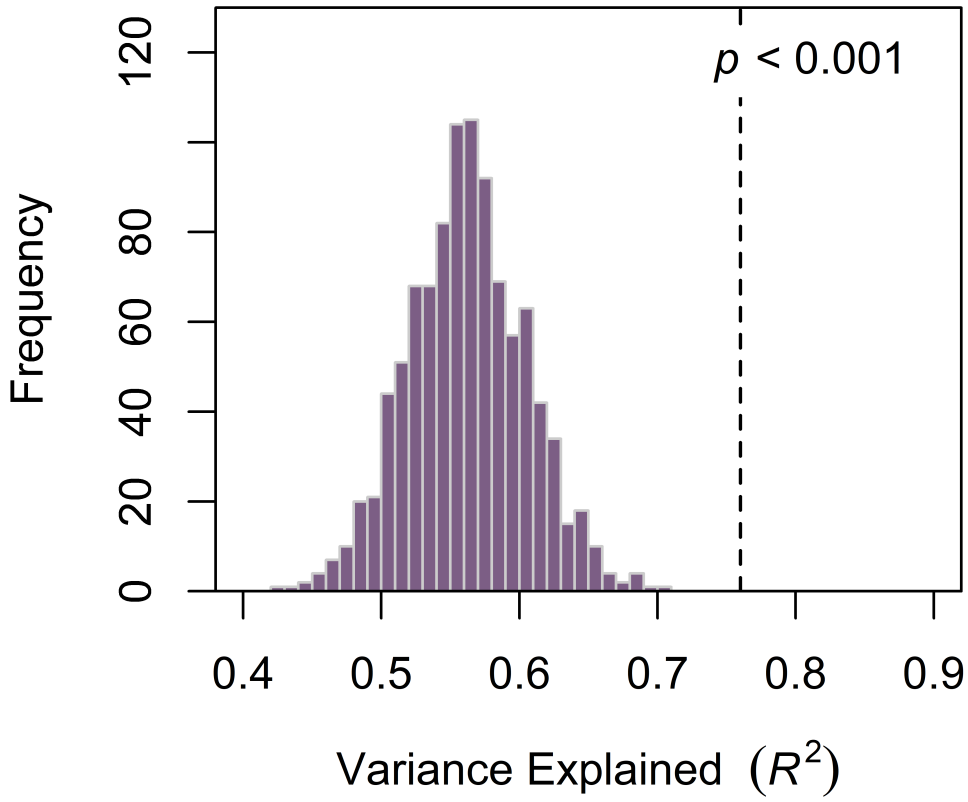

Figure S8. Results from the perMANOVA relating variation in cyanobiont partners to mycobionts' phylogenetic aafiliation. This analysis aims at explaining the variation in cyanobionts dissimilarity matrix among thalli (taking into account cyanobionts' genetic distances, not just phylogroup identity). The *x*-axis represents the percent vaiation in this dissimilarity matrix that can be explained by mycobionts' phylogenetic distance (i.e., tp what extent related mycobionts share similar cyanobionts). The dashed line represents the observed data (76% variation explained), and the purple histogram represents the values of 1000 randommatrices generated by constraining interactions only using geographical overlap between mycobionts and cyanobionts. None of our 1000 null matrices reach the 76% variation explained in the cyanobionts' dissimilarity matrix ($P < 0.00021$).

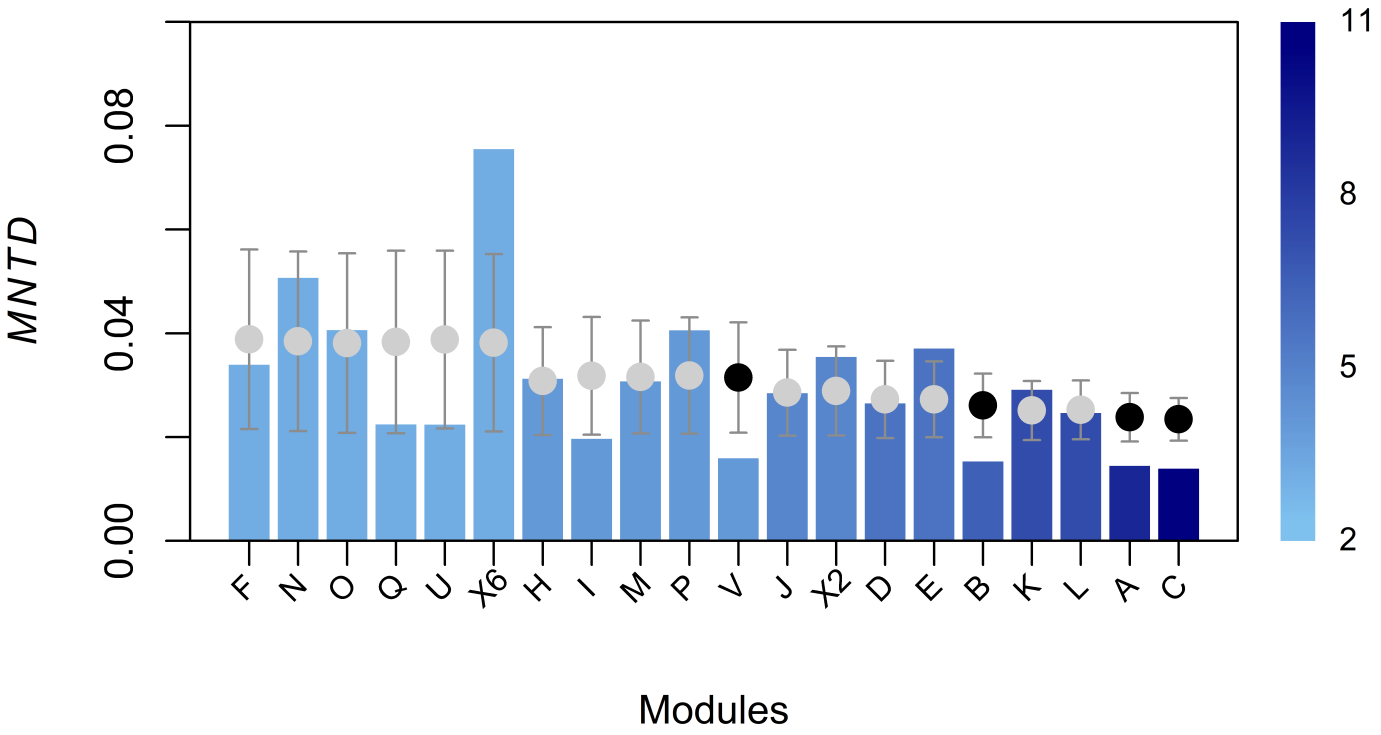

Figure S9. Phylogenetic clustering within modules for cyanobionts. The identity of the module (see Fig 1) is shown on the *x*-axis. The bars represent the calculated mean nearest taxon distance (*MNTD*) for each respective module, while the points represent the null expectations for the same module (±1SD). Black symbols indicate significant phylogenetic clustering (*MNTD* lower than null expectations) while grey symbols indicate non-significant trends. The color shade of the bars indicates the size of the module, i.e. the number of cyanobionts per module.